





Cite this: *Soft Matter*, 2019, 15, 9468

Oligo(ethylene glycol) side chain effect on the physical properties and molecular arrangement of oligothiophene–isoindigo based conjugated polymers†

Chien-An Chen,^a Shih-Chieh Wang,^b Shih-Huang Tung ^{*a} and Wei-Fang Su ^{*b}

Oligo(ethylene glycol) (OEG) side chains are widely used in donor–acceptor conjugated polymers (D–A CPs) and enable the polymers to dissolve and be processed in environmentally friendly and cost-effective nonchlorinated solvents, such as water. However, the OEG effect on the physical properties of D–A CPs has not been thoroughly studied and sometimes the results are controversial. In this study, two oligothiophene–isoindigo based conjugated polymers, P3TI and P4TI, are selected as model polymers to investigate the OEG effect. PnTI has octyl side chains on the oligothiophene unit and 2-hexyldecyl side chains on the isoindigo unit. The replacement of an alkyl side chain with OEG not only changes the optical and thermal properties but also the molecular arrangements of the polymers such as π – π *d*-spacing, crystallinity, and packing orientation. The domination of the crystallization behavior changes from the oligothiophene unit to the isoindigo unit when the bulky alkyl group is replaced by the flexible and linear OEG. The packing changes from edge-on to face-on orientation. The results are intriguing and provide new insights into this class of polymers.

Received 19th July 2019,
Accepted 29th October 2019

DOI: 10.1039/c9sm01471c

rsc.li/soft-matter-journal

Introduction

The donor–acceptor conjugated polymers (D–A CPs) have low bandgap, broad ultraviolet-visible (UV-Vis) absorption, and high conductivity, so they are widely used in polymer solar cells (PSCs),^{1,2} organic field-effect transistors (OFETs),^{3,4} and sensors.^{5,6}

The D–A CPs contain stiff and conjugated aromatic rings as well as flexible and insulated side chains. Although the side chains are insulated, they enable the D–A CPs to be dissolved in solvents and help the packing of the polymer molecules. Side chain engineering is utilizing side chains to improve the optoelectronic properties of D–A CPs for high performance devices.^{7,8} Many types of side chain have been used in D–A CPs, such as alkyl side chains,^{9,10} ionic side chains,^{11,12} hybrid side chains,^{13,14} oligo(ethylene glycol) (OEG) side chains,^{15,16} fluoroalkyl side chains,^{17,18} and so on. In the past ten years, the OEG side chain has gained lots of attention due to its flexibility and high polarity which enables the polymer to be dissolved in environment-friendly nonchlorinated solvents, such as water.^{19,20}

The OEG side chain effect on the properties of D–A CPs has not been extensively studied and sometimes the results are controversial. Many studies indicate that OEG shortens the distance of π – π stacking ($d_{\pi-\pi}$) of polymers, and thus enhances the crystallinity of the polymer and improves the device performance by replacing the bulky alkyl side chain with OEG.^{16,21–23} However, Mei and You *et al.* indicate that although OEG reduces the $d_{\pi-\pi}$ of polymers, it deteriorates the crystallinity of the polymers and the device performance.^{24,25} These studies encouraged us to elucidate the OEG effect on the properties of D–A CPs and find out how OEG influences the physical properties, especially the crystallinity and molecular arrangement of the polymers.

We chose two oligothiophene–isoindigo based conjugated polymers, P3TI and P4TI, as model polymers to systematically study the OEG side chain effect. The PnTI polymers are significant in the following respects: (1) isoindigo is a natural dye, and it can be extracted from plants and renewable resources,²⁶ (2) PnTI has good device performance (OFET: $\mu_{\text{h}} \sim 1 \text{ cm}^2 \text{ V}^{-1} \text{ s}^{-1}$; PSC: power conversion efficiency $\sim 8\%$),^{27,28} (3) PnTI is easy to synthesize,²⁹ and (4) PnTI is stable in air.⁵ In addition, bulky alkyl side chains are usually attached on the isoindigo unit of PnTI polymers to ensure the polymers have good solubility, and flexible OEG side chains are suitable for replacing the bulky alkyl side chains on the isoindigo unit to reduce the $d_{\pi-\pi}$ of the polymers. For P3TI and P4TI model polymers, octyl side chains

^a Institute of Polymer Science and Engineering, National Taiwan University, Taipei, 10617, Taiwan. E-mail: shtung@ntu.edu.tw

^b Department of Materials Science and Engineering, National Taiwan University, Taipei, 10617, Taiwan. E-mail: suwf@ntu.edu.tw

† Electronic supplementary information (ESI) available. See DOI: 10.1039/c9sm01471c

are installed on the oligothiophene unit, and 2-hexyldecyl side chains are placed on the isoindigo unit. We sequentially replaced the alkyl side chains with OEG side chains and systematically studied the changes of physical properties in the polymers. The 2-hexyldecyl side chains on the isoindigo unit are replaced by OEG side chains at first. Then, the octyl side chains on the oligothiophene unit are also replaced by OEG side chains. The effects of the partial and full replacement of the alkyl groups with OEG on the optical absorption, thermal properties, and molecular arrangement of the polymers are thoroughly investigated. The results are interesting and discussed below.

Results and discussion

A series of P3TI and P4TI polymers containing different amounts and location of oligo(ethylene glycol) (OEG) side chains were synthesized. Their structures are shown in Scheme 1. They are named as P3T(R₈)I(R_{b-16}), P3T(R₈)I(E), P3T(E)I(E), P4T(R₈)I(R_{b-16}), P4T(R₈)I(E), and P4T(E)I(E), where R₈, R_{b-16}, and E represent octyl, branched 2-hexyldecyl, and OEG, respectively. Note that OEG introduced in this work, *i.e.* tetraethylene glycol (TEG), cannot attach on the oligothiophene unit directly and the use of thiophene-3-ylmethanol to react with TEG is necessary. Therefore, OEG on the oligothiophene unit has one OCH₂ unit longer than the OEG on the isoindigo unit. Methoxy-TEG is expected to have similar properties as TEG in terms of flexibility, hydrophilicity, and so on. To simplify the discussion, OEG is used to represent either methoxy-TEG or TEG. The results of the synthesis, characterization, and molecular arrangement of the polymers are presented below and discussed in detail.

Polymer synthesis

P n TI polymers were synthesized by Stille coupling. The purity of the monomers was over 95% determined by ¹H nuclear magnetic resonance (¹H NMR), and thus polymers with high molecular weights (>10 kDa) were obtained. The molecular weights of the synthesized polymers were measured by gel permeation chromatography (GPC). The results are summarized in Table 1. To avoid the molecular weight effect in this study, we synthesized

Table 1 Summary of the molecular weight and optical property of the P n TI polymers

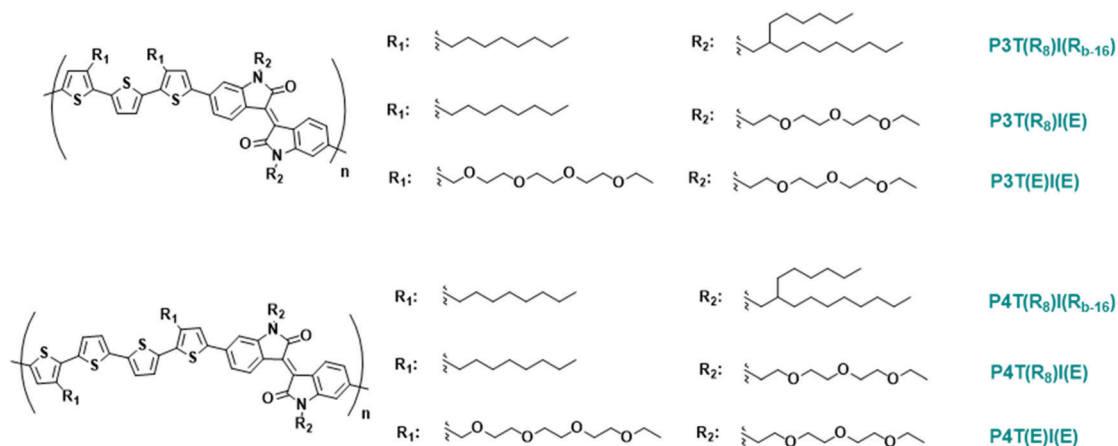
Polymer	M_n^a (kDa)	PDI ^a	λ_{\max}^b (nm)	$\lambda_{\text{shoulder}}^b$ (nm)	$E_g^{\text{opt}c}$ (eV)
P3T(R ₈)I(R _{b-16})	12.7	2.24	660	710	1.54
P3T(R ₈)I(E)	19.7	2.16	678	733	1.48
P3T(E)I(E)	13.3	2.05	639	—	1.56
P4T(R ₈)I(R _{b-16})	18.9	2.34	644	705	1.61
P4T(R ₈)I(E)	12.2	2.54	669	720	1.51
P4T(E)I(E)	14.9	2.03	646	—	1.54

^a Molecular weights estimated from GPC using polystyrene standard, chloroform as eluent, at 40 °C. ^b UV-Vis absorption spectra of the films spun-cast from 10 mg ml⁻¹ chloroform solutions then annealed at 200 °C for 1 h. ^c Optical bandgaps calculated from the absorption edge (onset of the peak) of UV-Vis spectra.

the polymers with similar molecular weights in the range of 12–20 kDa. The detailed synthesis scheme of the P n TI polymers is shown in the ESI.†

OEG effects on optical properties

Fig. 1 displays the absorption spectra of annealed P n TI films. All of the polymers show broad dual band absorption between 300 and 850 nm. λ_{\max} between 600 and 700 nm and $\lambda_{\text{shoulder}}$ between 700 and 800 nm are contributed from intramolecular charge transfer (ICT) and intermolecular π - π stacking, respectively. The intensity of the $\lambda_{\text{shoulder}}$ is related to the packing of polymer chains and closely correlated with the crystallinity.³⁰ The values of λ_{\max} , $\lambda_{\text{shoulder}}$, and the calculated optical bandgap are listed in Table 1. For P3TI polymers, P3T(R₈)I(R_{b-16}) shows a clear $\lambda_{\text{shoulder}}$, implying that P3T(R₈)I(R_{b-16}) has a high extent of π - π stacking and high crystallinity. As R_{b-16} was replaced by OEG on the isoindigo unit, *i.e.* P3T(R₈)I(E), λ_{\max} red-shifts from 660 nm to 678 nm, but no clear $\lambda_{\text{shoulder}}$ is observed. The results indicate that flexible, linear OEG on the isoindigo unit may shorten the distance of π - π stacking of the polymer to have a red-shift of λ_{\max} . However, the crystallinity of the polymer is decreased. Further replacing R₈ on the oligothiophene unit with OEG, *i.e.* P3T(E)I(E), $\lambda_{\text{shoulder}}$ disappears and λ_{\max} blue-shifts from 678 nm to 639 nm. The results show that OEG on the oligothiophene unit further decreases the crystallinity



Scheme 1 Chemical structures of P n TI polymers.

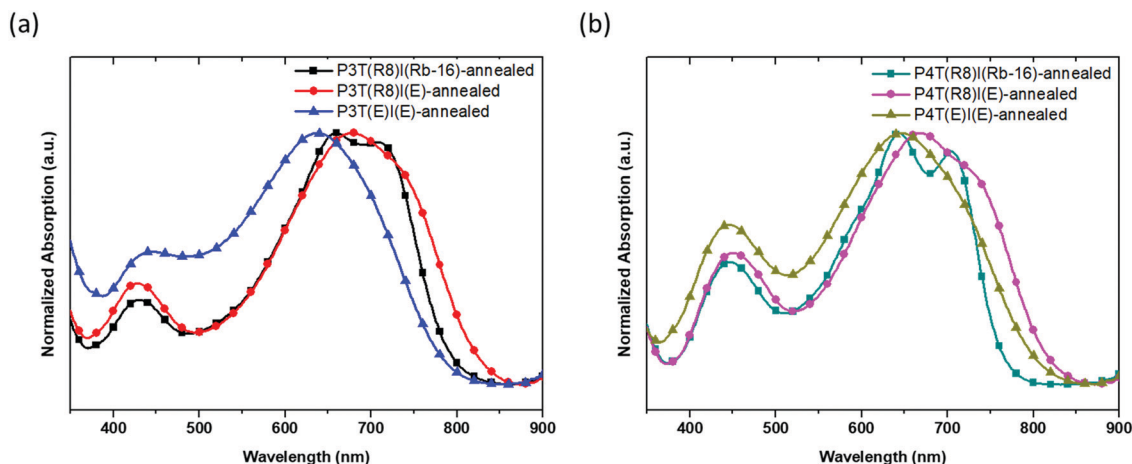


Fig. 1 UV-Vis absorption spectra of (a) P3TI and (b) P4TI thin films spun-cast from 10 mg ml⁻¹ chloroform solutions, then annealed at 200 °C for 1 h.

of the polymer. Similar results can also be found in P4TI polymers. The crystallinity of the polymer affected by OEG substitution plays a critical role in the packing orientation of the polymer chains, which will be discussed later.

OEG effects on thermal properties

Fig. 2 shows the TGA and DSC profiles of the P_nTI polymers. The degradation temperature T_d and the melting temperature T_m are summarized in Table 2. The TGA profiles reveal that the polymers with all alkyl side chains, P3T(R₈)I(R_{b-16}) and P4T(R₈)I(R_{b-16}), exhibit the highest T_d in their respective series of polymers. After the replacement of R_{b-16} with OEG on the isoindigo unit, the T_d of P3T(R₈)I(E) and P4T(R₈)I(E) are slightly reduced by 5–9 °C. However, after the further replacement of R₈ with OEG on the oligothiophene unit, the T_d of P3T(E)I(E) and P4T(E)I(E) are greatly reduced by 101–115 °C as compared with their alkyl analogues. The large decrease in the thermal stability is because the oxygen atoms on OEG tend to form oxygen radicals at high temperature and promote radical chain decomposition reaction.

Table 2 Thermal properties of P_nTI polymers

Polymer	T_d (°C)	T_m (°C)
P3T(R ₈)I(R _{b-16})	352	268
P3T(R ₈)I(E)	347	—
P3T(E)I(E)	251	—
P4T(R ₈)I(R _{b-16})	359	307
P4T(R ₈)I(E)	350	299
P4T(E)I(E)	244	—

The DSC profiles reveal the crystallization behavior of the polymers. For P3TI polymers, only P3T(R₈)I(R_{b-16}) shows a sharp melting peak at 268 °C and no melting peak is observed for the polymers with OEG side chains before thermal degradation. For P4TI polymers, P4T(R₈)I(R_{b-16}) shows a sharper melting peak at a higher temperature of 307 °C while the melting peak of P4T(R₈)I(E) is broader and at a lower temperature of 299 °C. The melting peak is absent for P4T(E)I(E) before degradation. These results indicate that the OEG side chains inhibit the crystallization of the P_nTI polymers, consistent with the UV-Vis absorption spectra shown in Fig. 1. In the case of the higher

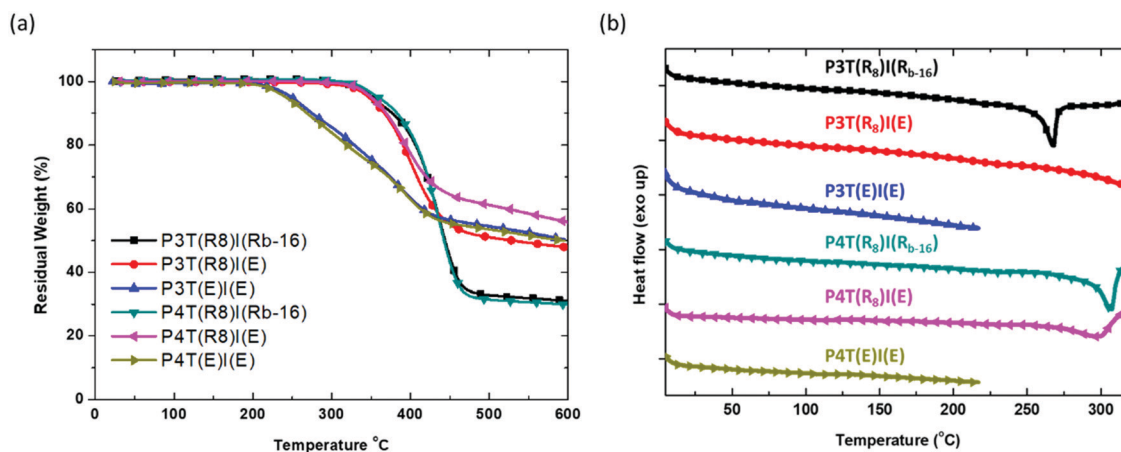


Fig. 2 (a) TGA profiles and (b) DSC profiles of P_nTI polymers.

crystallinity polymers, P3T(R₈)I(R_{b-16}) and P4T(R₈)I(R_{b-16}), considering that the bulky branched side chains (R_{b-16}) can prohibit the close packing of the isoindigo units, the crystallization of the polymers should be dominantly driven by the oligothiophene unit that bears smaller side chains (R₈). This can also be supported by the fact that the T_m of P4T(R₈)I(R_{b-16}) with more thiophene units is higher than that of P3T(R₈)I(R_{b-16}) even though they have the same isoindigo unit.³¹ The decrease in crystallinity upon replacing the alkyl side chains on isoindigo with OEG is because the small size of the linear OEG side chains allows the isoindigo unit to be more closely packed, which may slightly shift the relative positions of the polymer backbones and in turn sacrifice the original stable packing of the oligothiophene unit. This argument can be verified by the change in π - π d -spacing upon the incorporation of OEG chains as shown in the GIWAXS study below.

OEG effects on the thin film morphology

Fig. 3 shows the 2D-GIWAXS patterns of the P n TI thin films. The polymer films were annealed at 200 °C for 1 h to ensure that the morphology of the polymer films is thermodynamically stable. All P4TI polymers show a highly ordered lamellar structure with clear multiple scattering peaks at a q ratio of 1 : 2 : 3. The scattering peak contributed from π - π stacking can also be observed. In contrast, P3TI polymers only show a clear first-order scattering peak from lamellae, along with a π - π stacking scattering. The results are attributed to the shape and coplanarity of the polymer chains. The molecular conformation of the D-A unit of the polymer was simulated using Gaussian 9.0 software as shown in Fig. S1 and Table S2 (ESI†). The linear and planar backbones of the P4TI polymers can stack into a more ordered lamellar structure. In contrast, the S-shaped and twisted backbones of the P3TI polymers are not suitable for lamellar stacking.

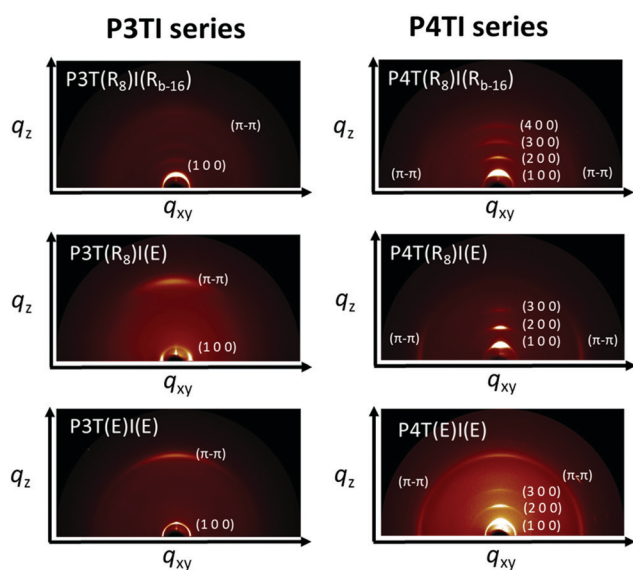


Fig. 3 2D-GIWAXS patterns of annealed P n TI films which were drop-cast from 10 mg mL⁻¹ chloroform solutions, then annealed at 200 °C for 1 h.

Fig. 4a and b show the line cut data along the q_z -axis and the q_{xy} -axis, from which the d -spacing of the lamellar stacking d_L and the π - π stacking $d_{\pi-\pi}$ can be estimated. The calculated d_L and $d_{\pi-\pi}$ are listed in Table 3. The d_L values of the P3TI polymers (19.4–20.9 Å) are larger than those of P4TI polymers (16.2–18.0 Å), which is attributed to the radially wider S-shaped P3TI backbone. For both P3TI and P4TI polymers, the replacement of R_{b-16} with OEG on isoindigo reduces d_L , from 20.9 Å to 19.4 Å and from 18.0 Å to 16.2 Å for P3TI and P4TI respectively. The OEG side chain may need to interdigitate or laterally coil between the backbones to attain uniform segmental density in the side chain layer, thereby leading to a reduction of d_L . Further replacing the R₈ with OEG on oligothiophene increases d_L to 20.3 Å and 18.0 Å respectively, due to the longer length of the OEG chains compared to R₈ chains.

The effect of OEG on $d_{\pi-\pi}$ is similar for both P3TI and P4TI polymers, and the change is intriguing. We have shown that the crystallinity of both P3TI and P4TI polymers decreases when more OEG chains are incorporated into P n TIs by DSC study (Fig. 2b), but surprisingly, the scattering peaks of the π - π stacking become sharper and $d_{\pi-\pi}$ decreases when OEG chains are attached on the isoindigo unit (Fig. 4a and b). For the P3TI polymers, $d_{\pi-\pi}$ is reduced from 3.92 Å of P3T(R₈)I(R_{b-16}) to 3.57 Å of P3T(R₈)I(E) and P3T(E)I(E). For the P4TI polymers, $d_{\pi-\pi}$ is reduced from 3.92 Å to 3.61 Å. As mentioned earlier, in the case of P3T(R₈)I(R_{b-16}) and P4T(R₈)I(R_{b-16}), the isoindigo unit cannot closely pack due to the large steric hindrance of the bulky branched R_{b-16}. The packing of the P3T(R₈)I(R_{b-16}) and P4T(R₈)I(R_{b-16}) chains is therefore dominated by the oligothiophene unit and the $d_{\pi-\pi}$ spacing of 3.92 Å happens to be close to that of poly(3-alkylthiophene), \sim 3.87 Å.³² Once isoindigo units are grafted with linear OEG, the packing of the isoindigo units becomes dominant regardless of the type of side chain on the oligothiophenes, which thus gives a $d_{\pi-\pi}$ of 3.57–3.61 Å close to that of 3.65 Å for isoindigo oligomers.³³ Note that although the isoindigo unit with linear OEG chains can control the packing of P n TI polymers, they are unable to cause the crystallization of the polymer chains. Instead, their close packing deteriorates the crystallization of the oligothiophene unit, as shown by the DSC profiles in Fig. 2b. In other words, the crystallization of P n TI is driven by the oligothiophene unit, not the isoindigo unit.

OEG effects on packing orientations

The packing orientation in P n TI films can be determined from the 2D-GIWAXS as shown in Fig. 3. Fig. 4 illustrates line cut data and the pole figures based on the intensity of the first-order (100) scattering as a function of the azimuthal angle. A stronger (100) peak on the q_z -axis than on the q_{xy} -axis in Fig. 4a and b, and a stronger (100) intensity around 90° in the pole figures of Fig. 4c indicate a preference for edge-on orientation, which can also be determined from a stronger π - π stacking peak on the q_{xy} -axis than on the q_z -axis. The opposite results indicate a preference for face-on orientation. For P3TI polymers, the replacement of alkyl side chains with OEG dramatically transforms the slightly edge-on orientation of P3T(R₈)I(R_{b-16}) to the highly face-on orientation of P3T(R₈)I(E) and P3T(E)I(E)

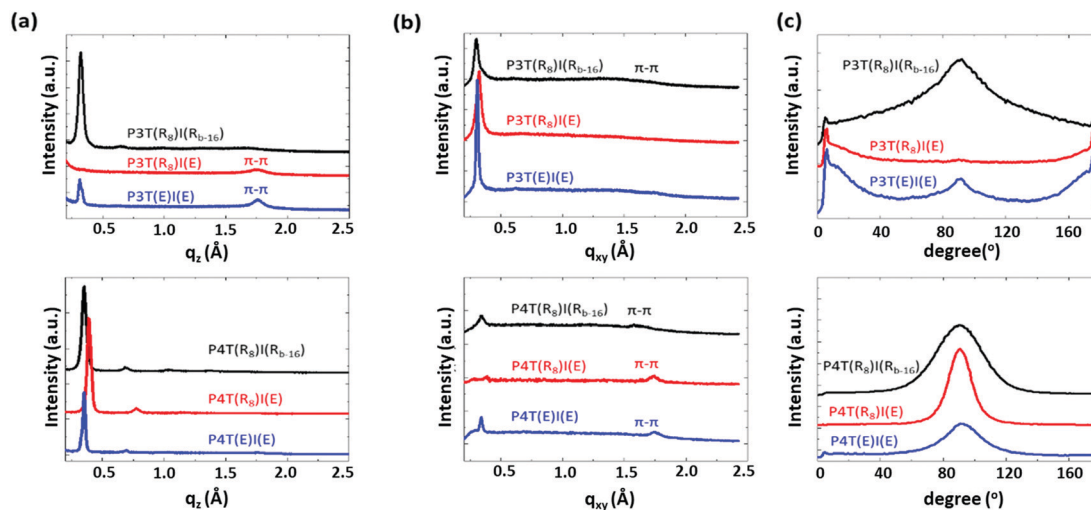


Fig. 4 (a) Line cut data of the z-axis, (b) line cut data of the xy-axis, and (c) pole figures of the primary peak (100) extracted from the 2D-GIWAXS patterns in Fig. 3.

Table 3 Summary of the GIWAXS parameters of annealed P n TI films

Polymer	Peak ratio	d_L (Å)	$d_{\pi-\pi}$ (Å)	Orientation
P3T(R ₈)I(R _{b-16})	1	20.9	3.92	Slightly edge-on
P3T(R ₈)I(E)	1	19.4	3.57	Face-on
P3T(E)I(E)	1	20.3	3.57	Face-on
P4T(R ₈)I(R _{b-16})	1 : 2 : 3 : 4	18.0	3.92	Edge-on
P4T(R ₈)I(E)	1 : 2 : 3	16.2	3.61	Edge-on
P4T(E)I(E)	1 : 2 : 3	18.0	3.61	Mixed

where a clear scattering of π - π stacking appears in the q_z direction. For P4TI polymers, the effect of OEG side chains is not as pronounced as in P3TI polymers, from the highly ordered edge-on arrangement of P4T(R₈)I(R_{b-16}) and P4T(R₈)I(E) to a mixed arrangement of P4T(E)I(E) where some face-on feature appears. The orientations of the films are summarized in Table 3.

In thin films, the conjugated polymers with strong intermolecular interactions, especially the backbone π - π interactions, generally show a high crystallinity and tend to arrange in the edge-on fashion to extend the range of the ordered packing in the in-plane direction.³⁴ Another critical factor that influences the packing orientation of polymers is the backbone conformation. It has been shown that in order to closely contact the substrate, the polymers with S-shape backbones prefer to pack with the face-on orientation while the polymers with linear backbones favor the edge-on orientation.³⁴ By combining these two factors, we can explain the orientation of P3TI and P4TI thin films as follows. The backbones of P3TI polymers are S-shaped and the face-on orientation is naturally favorable. However, the high crystallinity of P3T(R₈)I(R_{b-16}) may significantly influence the packing and thus the edge-on orientation is slightly preferred in this case. For P3T(R₈)I(E) and P3T(E)I(E), the introduction of an OEG side chain decreases the crystallinity. Therefore, the S-shaped backbones become dominant and the polymers are forced to adopt the face-on orientation. The backbones of P4TI polymers are linear so that the edge-on orientation is inherently favorable. Along with the crystalline nature, P4T(R₈)I(R_{b-16}) and

P4T(R₈)I(E) thin films are as expected highly edge-on oriented while the nearly suppressed crystallization allows P4T(E)I(E) to reveal some face-on features. These results indicate that OEG side chains are capable of controlling the packing orientation of P n TI polymers in thin films by altering the intermolecular interactions.

Conclusions

We successfully synthesized a series of P3TI and P4TI polymers by varying the number and location of oligo(ethylene glycol) (OEG) side chains. Their optical properties, thermal properties, and morphologies are systematically studied. High crystallization capability of P n TI polymers is mainly contributed from the stable stacking of the oligothiophene unit. For the polymers with all alkyl side chains, P3T(R₈)I(R_{b-16}) and P4T(R₈)I(R_{b-16}), they show the highest crystallinity but the largest $d_{\pi-\pi}$ among each series of polymers. Their π - π stacking behavior is dominated by the oligothiophene unit because the bulky alkyl side chains (R_{b-16}) on the isoindigo unit prohibit the close packing of the isoindigo unit. As the bulky R_{b-16} side chains on the isoindigo unit are replaced by linear and flexible OEG side chains, *i.e.* P3T(R₈)I(E), P3T(E)I(E), P4T(R₈)I(E), and P4T(E)I(E), their π - π stacking behavior is dominated by the isoindigo unit because the isoindigo unit with a small size of the OEG side chains can stack more closely than the oligothiophene unit, resulting in a sacrifice for stable stacking of the oligothiophene unit. Therefore, even though they show relatively short $d_{\pi-\pi}$, their crystallinity is relatively low. In our opinion, OEG side chains can alter the π - π stacking behavior of the polymer chains to influence the crystallinity of the polymers, especially for donor-acceptor conjugated polymers. In addition, OEG side chains are capable of controlling the packing orientation of the polymers by adjusting the crystallinity of the polymers. For instance, OEG side chains change the packing orientation of P3TI polymers from slightly edge-on orientation of P3T(R₈)I(R_{b-16}) to

fully face-on orientation of P3T(R₈)I(E) and P3T(E)I(E) which is suitable for polymer solar cell applications.

Conflicts of interest

There are no conflicts to declare.

Acknowledgements

The authors thank the Ministry of Science and Technology of Taiwan (107-2221-E-002-005, 108-2221-E-002-027-MY3, 107-3017-F-002-001) and the Ministry of Education (107L9006) for the financial support of this research and the National Synchrotron Radiation Research Center of Taiwan for providing the GIWAXS instrument.

References

- Q. Fan, Y. Wang, M. Zhang, B. Wu, X. Guo, Y. Jiang, W. Li, B. Guo, C. Ye, W. Su, J. Fang, X. Ou, F. Liu, Z. Wei, T. C. Sum, T. P. Russell and Y. Li, *Adv. Mater.*, 2018, **30**, 1704546.
- C. Sun, F. Pan, H. Bin, J. Zhang, L. Xue, B. Qiu, Z. Wei, Z.-G. Zhang and Y. Li, *Nat. Commun.*, 2018, **9**, 743.
- I. Kang, H.-J. Yun, D. S. Chung, S.-K. Kwon and Y.-H. Kim, *J. Am. Chem. Soc.*, 2013, **135**, 14896–14899.
- T. Lei, J.-H. Dou, Z.-J. Ma, C.-H. Yao, C.-J. Liu, J.-Y. Wang and J. Pei, *J. Am. Chem. Soc.*, 2012, **134**, 20025–20028.
- C.-F. Lu, C.-W. Shih, C.-A. Chen, A. Chin and W.-F. Su, *Adv. Funct. Mater.*, 2018, **28**, 1803145.
- D. Khim, G.-S. Ryu, W.-T. Park, H. Kim, M. Lee and Y.-Y. Noh, *Adv. Mater.*, 2016, **28**, 2752–2759.
- H. Huang, H. Bin, Z. Peng, B. Qiu, C. Sun, A. Liebman-Pelaez, Z.-G. Zhang, C. Zhu, H. Ade, Z. Zhang and Y. Li, *Macromolecules*, 2018, **51**, 6028–6036.
- J. Mei and Z. Bao, *Chem. Mater.*, 2014, **26**, 604–615.
- C. Piliago, T. W. Holcombe, J. D. Douglas, C. H. Woo, P. M. Beaujuge and J. M. J. Fréchet, *J. Am. Chem. Soc.*, 2010, **132**, 7595–7597.
- L. Zhu, C. Jiang, G. Chen, Z. Zhou and Q. Li, *Org. Electron.*, 2017, **49**, 278–285.
- J. H. Seo, A. Gutacker, B. Walker, S. Cho, A. Garcia, R. Yang, T.-Q. Nguyen, A. J. Heeger and G. C. Bazan, *J. Am. Chem. Soc.*, 2009, **131**, 18220–18221.
- A. Duarte, K.-Y. Pu, B. Liu and G. C. Bazan, *Chem. Mater.*, 2011, **23**, 501–515.
- C. Shi, Y. Yao, Y. Yang and Q. Pei, *J. Am. Chem. Soc.*, 2006, **128**, 8980–8986.
- X. Guo, J. Quinn, Z. Chen, H. Usta, Y. Zheng, Y. Xia, J. W. Hennek, R. P. Ortiz, T. J. Marks and A. Facchetti, *J. Am. Chem. Soc.*, 2013, **135**, 1986–1996.
- S.-F. Yang, Z.-T. Liu, Z.-X. Cai, M. J. Dyson, N. Stingelin, W. Chen, H.-J. Ju, G.-X. Zhang and D.-Q. Zhang, *Adv. Sci.*, 2017, **4**, 1700048.
- B. Meng, H. Song, X. Chen, Z. Xie, J. Liu and L. Wang, *Macromolecules*, 2015, **48**, 4357–4363.
- M.-H. Lee, M. Kang, H.-G. Jeong, J.-J. Park, K. Hwang and D.-Y. Kim, *Macromol. Rapid Commun.*, 2018, **39**, 1800431.
- B. Kang, R. Kim, S. B. Lee, S.-K. Kwon, Y.-H. Kim and K. Cho, *J. Am. Chem. Soc.*, 2016, **138**, 3679–3686.
- M. Shao, Y. He, K. Hong, C. M. Rouleau, D. B. Geohegan and K. Xiao, *Polym. Chem.*, 2013, **4**, 5270–5274.
- Z. Chen, L. Yan, J. J. Rech, J. Hu, Q. Zhang and W. You, *ACS Appl. Polym. Mater.*, 2019, **1**, 804–814.
- X. Chen, Z. Zhang, J. Liu and L. Wang, *Polym. Chem.*, 2017, **8**, 5496–5503.
- X. Chen, Z. Zhang, Z. Ding, J. Liu and L. Wang, *Angew. Chem., Int. Ed.*, 2016, **55**, 10376–10380.
- C. Kanimozhi, N. Yaacobi-Gross, E. K. Burnett, A. L. Briseno, T. D. Anthopoulos, U. Salzner and S. Patil, *Phys. Chem. Chem. Phys.*, 2014, **16**, 17253–17265.
- X. Zhao, G. Xue, G. Qu, V. Singhania, Y. Zhao, K. Butrouna, A. Gumyusenge, Y. Diao, K. R. Graham, H. Li and J. Mei, *Macromolecules*, 2017, **50**, 6202–6209.
- S. Zhang, J. Gao, W. Wang, C. Zhan, S. Xiao, Z. Shi and W. You, *ACS Appl. Energy Mater.*, 2018, **1**, 1276–1285.
- D. Wang, W. Ying, X. Zhang, Y. Hu, W. Wu and J. Hua, *Dyes Pigm.*, 2015, **112**, 327–334.
- C.-C. Ho, C.-A. Chen, C.-Y. Chang, S. B. Darling and W.-F. Su, *J. Mater. Chem. A*, 2014, **2**, 8026–8032.
- T. Lei, Y. Cao, Y. Fan, C.-J. Liu, S.-C. Yuan and J. Pei, *J. Am. Chem. Soc.*, 2011, **133**, 6099–6101.
- E. Wang, Z. Ma, Z. Zhang, K. Vandewal, P. Henriksson, O. Inganäs, F. Zhang and M. R. Andersson, *J. Am. Chem. Soc.*, 2011, **133**, 14244–14247.
- H.-C. Liao, C.-P. Hsu, M.-C. Wu, C.-F. Lu and W.-F. Su, *Anal. Chem.*, 2013, **85**, 9305–9311.
- W. Elsbary, C.-L. Lee, S. Cho, S.-H. Oh, S.-H. Moon, A. Elbarbary and J.-S. Lee, *Phys. Chem. Chem. Phys.*, 2013, **15**, 15193–15203.
- R. J. Kline, M. D. McGehee, E. N. Kadnikova, J. Liu, J. M. J. Fréchet and M. F. Toney, *Macromolecules*, 2005, **38**, 3312–3319.
- Y. Ren, A. M. Hiszpanski, L. Whittaker-Brooks and Y.-L. Loo, *ACS Appl. Mater. Interfaces*, 2014, **6**, 14533–14542.
- I. Osaka and K. Takimiya, *Polymer*, 2015, **59**, A1–A15.